Çukurova Üniversitesi Mühendislik Fakültesi Dergisi
Çukurova University Journal of the Faculty of Engineering
ISSN: 2757-9255 CİLT/VOLUME: 41 SAYI/ISSUE: 2 HAZİRAN/JUNE 2026

Design and Performance Analysis of Tulip-Shaped Microstrip Antenna on Flexible Substrates with Chemical Modifications

Mustafa Berkan BİÇER [1,a], Emine AVŞAR AYDIN [2,b], Mehmet Erman MERT [3,c], Başak DOĞRU MERT [4,d]

[1]*Tarsus University, Faculty of Engineering, Department of Electrical-Electronics Engineering, Mersin, Türkiye*
[2]*Adana Alparslan Türkeş Science and Technology University, Faculty of Computer and Informatics, Department of Information Systems and Technologies, Adana, Türkiye*
[3]*Adana Alparslan Türkeş Science and Technology University, Advanced Technology Research and Application Center, Adana, Türkiye*
[4]*Adana Alparslan Türkeş Science and Technology University, Faculty of Engineering, Department of Energy Systems Engineering, Adana, Türkiye*

[a]***ORCID***: *0000-0003-3278-6071;* [b]***ORCID***: *0000-0002-5068-2957;* [c]***ORCID***: *0000-0002-0114-8707;* [d]***ORCID***: *0000-0002-2270-9032*

Article Info
Received : 31.12.2025
Accepted : 25.03.2026
DOI: 10.21605/cukurovaumfd.1852865

Corresponding Author
Emine AVŞAR AYDIN
eaydin@atu.edu.tr

Keywords
Tulip-shaped
Microstrip antenna
Reflection coefficient
Chemical process

How to cite: *BİÇER, M.B., AVŞAR AYDIN, E., MERT, M.E., DOĞRU MERT, B., (2026). Design and Performance Analysis of Tulip-Shaped Microstrip Antenna on Flexible Substrates with Chemical Modifications. Cukurova University, Journal of the Faculty of Engineering, 41(2), 309-319.*

ABSTRACT

This study introduces a novel tulip-shaped microstrip antenna (TSMA), fabricated on a chemically analyzed substrate with versatile applications. The antenna design is implemented using Computer Simulation Tool (CST) software, considering various substrate materials. Performance analyses, including reflection coefficients and voltage standing wave ratio graphs, are presented for each material. The antennas exhibit diverse characteristics, with some featuring wide bandwidths, others narrow bands, and some offering dual or tri-band resonances—tailored for specific application areas. The production costs remain reasonable, leveraging the benefits of chemical processes and material flexibility. Simulation results validate the study's findings, highlighting the antennas' simple, compact structures and cost-effectiveness, making them suitable for tailored RF applications.

Kimyasal Modifikasyonlu Esnek Altlıklar Üzerinde Lale Şekilli Mikroşerit Antenin Tasarımı ve Performans Analizi

Makale Bilgileri
Geliş : 31.12.2025
Kabul : 25.03.2026
DOI: 10.21605/cukurovaumfd.1852865

Sorumlu Yazar
Emine AVŞAR AYDIN
eaydin@atu.edu.tr

Anahtar Kelimeler
Lale-şekilli
Mikroşerit anten
Yansıma katsayısı
Kimyasal işlem

Atıf şekli: *BİÇER, M.B., AVŞAR AYDIN, E., MERT, M.E., DOĞRU MERT, B., (2026). Kimyasal Modifikasyonlu Esnek Altlıklar Üzerinde Lale Şekilli Mikroşerit Antenin Tasarımı ve Performans Analizi. Çukurova Üniversitesi, Mühendislik Fakültesi Dergisi, 41(2), 309-319.*

ÖZ

Bu çalışma, çok yönlü uygulamalara sahip, kimyasal olarak analiz edilmiş bir taban malzeme üzerine üretilen yenilikçi bir lale şekilli mikroşerit anten (LŞMA) sunmaktadır. Anten tasarımı, çeşitli taban malzemeleri dikkate alınarak Computer Simulation Tool (CST) yazılımı kullanılarak gerçekleştirilmiştir. Her bir malzeme için yansıma katsayıları ve gerilim duran dalga oranı (VSWR) grafiklerini içeren performans analizleri sunulmuştur. Antenler; belirli uygulama alanlarına göre özelleştirilmiş olarak, bazıları geniş bant genişliğine, diğerleri dar bantlara sahip olan ve bazıları ise çift veya üçlü bant rezonansları sunan çeşitli karakteristikler sergilemektedir. Kimyasal süreçlerin ve malzeme esnekliğinin avantajlarından yararlanılarak üretim maliyetleri makul seviyelerde tutulmuştur. Simülasyon sonuçları, antenlerin basit, kompakt yapılarını ve maliyet etkinliğini vurgulayarak çalışmanın bulgularını doğrulamakta ve bu antenleri özelleştirilmiş RF uygulamaları için uygun hale getirmektedir.

1. INTRODUCTION

The utilization of antennas in electromagnetic applications is indispensable for the operation of radar systems, wireless communication, and other sensing technologies. Antennas play a crucial role in the transmission and reception of information through electromagnetic waves, enabling the propagation of information across extensive distances and powering numerous contemporary devices. Their significance stems from their ability to adeptly capture, propagate, and manipulate electromagnetic waves, forming the foundational basis for modern sensing and telecommunication networks. The progression of materials and antenna technologies tailored for electromagnetic applications is imperative for high-tech applications.

Using different substrates and conductive materials, numerous antenna studies and developments have been carried out, ranging from biomedical applications to space and satellite antenna systems [1, 2]. In [1], an ultra-wideband bow-tie antenna and a three-dimensional breast model with varied permittivity and conductivity were designed in CST to investigate microwave breast cancer detection. The study evaluated key antenna characteristics such as return loss and radiation pattern, and it further examined the influence of a limestone layer surrounding the tumor on the radiated electric and magnetic field distributions. The findings showed that limestone can significantly affect the field response and tumor visibility, emphasizing the importance of tissue composition in microwave-based diagnostic scenarios. In a seperate study [2], the researchers designed a frequency-configurable flexible horizontal H-shaped microstrip antenna for biomedical applications by using copper tape radiating and ground structures on felt, jean, and photographic paper substrates. The antennas were analyzed over the 2-10 GHz band with a full-wave solver based on the finite integration technique and were subsequently fabricated to compare measured and simulated responses. Their results demonstrated that flexible substrate selection and dielectric characteristics strongly influence impedance matching, bandwidth behavior, and the practical feasibility of low-cost biomedical microwave antenna implementations.

Researchers [3] have developed copper and nickel-plated polymethacrylimide composite foam (PMIF@Ni and PMIF@Cu) demonstrating high surface electrical conductivities, with values reaching 1.06 x 10^4 S/m and 9.15 x 10^3 S/m, respectively. These composite foams have exhibited noteworthy electromagnetic interface shielding effectiveness (EMI SE), registering approximately 52 dB for PMIF@Ni and approximately 43 dB for PMIF@Cu. Furthermore, the researchers have successfully employed these composite foams to fabricate monopole antennas operative within the frequency range of 0.9 GHz to 1.2 GHz, underscoring the material's suitability for electromagnetic purposes.

In a separate study [4], a nickel ferrite-based composite material was synthesized using the sol-gel method, offering tailored microwave absorption performance in the X-band. When applied as a coating on a metal sheet, the material manifested resonance dips at frequencies of 8.42 GHz, 9.5 GHz, and 10.80 GHz, indicating effective microwave absorption within the desired frequency range.

Similarly, researchers [5] explored the utilization of Ni/Ppy/PET conductive fabrics for electromagnetic interference shielding and wearable textile antenna applications. Comparative analysis within a specified frequency range (8.12 GHz to 12.4 GHz) validated the performance of the proposed composite fabric. Additionally, a wearable antenna application was developed, featuring a microstrip-fed patch antenna with a reflection loss of -32.08 dB at the 2.40 GHz frequency band, emphasizing its potential for practical implementation. Guerchouche et al. [6] formulated a design for a compact broadband RFID antenna intended for "Green" electronics and biosensor applications. This design employed transparent conductive films on recyclable substrates, highlighting the potential environmental sustainability of the proposed technology. The study emphasized the application viability of conductive polymers in proximity-based contactless technology. Jeon et al. [7] proposed a flexible monopole radio-frequency antenna utilizing a graphene/polymer nanocomposite film. Experimental results yielded reflection coefficient values ranging from -11.3 dB to -37.5 dB within the frequency range of 2.49 GHz to 2.77 GHz. Mechanical deformation tests underscored the antenna's flexibility, suggesting its suitability for integration into wireless communication technologies. Feili et al. [8] contributed by developing an antenna tailored for flexible wireless sensor systems, with specified numerical parameters including thickness (100 µm), dielectric constant (2.9), and loss tangent (0.002). The antenna, employing a liquid crystal polymer (LCP) substrate with a Cu-based metal film patch, underwent parametric studies, providing insights into optimizing its performance. Hasan et al. [9] introduced a nickel zinc ferrite thick film for microwave applications, illustrating its effectiveness through numerical data depicting improved reflection coefficients. The designed antenna exhibited a reflection coefficient of -29.33 dB at 5.64 GHz, highlighting the potential utility of the developed film in enhancing the performance of electromagnetic devices. Li et al. [10] developed nickel-modified zinc molybdate ceramics with a dielectric constant 8.5 and the product Q×f of 28192 GHz, demonstrating suitability for two-dimensional beam splitting of array antennas in the X-band. Kyovtorov et al. [11] introduced a novel prototyping method utilizing 3D printing and chemical metallization to produce a metal pyramidal horn antenna prototype, showcasing performance in the frequency range of 14-18 GHz. Anilkumar et al. [12] designed an antenna utilizing a liquid crystal polymer substrate, with operating frequencies ranging from 2.4 GHz to 12.5 GHz, optimized for automotive communication applications. Matyas et al. [13] developed a microstrip antenna using silver nanoparticles on a flexible PET foil, operating at frequencies of 2.02 GHz and 2.3 GHz with reflection coefficients of -16.02 dB and -19.33 dB, respectively. Sid et al. [14] devised a patch antenna tailored for wearable applications, operating at 2.45 GHz. They utilized cellulose laurate as a bio-based polymer substrate, characterized by a dielectric constant of 2.66 and a loss tangent of 0.025. In the realm of 5G mobile communication, Hwang et al. [15] designed vertically stacked dipole antennas for dual-band operation at 28/34 GHz. Employing a flexible liquid crystal polymer substrate, they achieved element gains of 4.8 dBi and 4.6 dBi at the respective frequencies.

Mohamadzade et al. [16] introduced a dynamic pattern-reconfigurable antenna design utilizing conductive textile-polymer composites, showcasing a -10 dB bandwidth spanning from 4.67 GHz to 5.59 GHz. Elobaid et al. [17] innovatively developed a transparent and flexible ultrawideband antenna by incorporating a transparent conductive fabric tissue on a PDMS substrate. This design achieved reflection coefficient values below -10 dB across a spectrum ranging from 2.5 GHz to 25 GHz. Hamouda et al. [18] formulated a dual-band flexible antenna specifically designed for wearables, utilizing a magnetodielectric nanocomposite polymer. This antenna exhibited promising performance, even in complex bending situations.

In this study, our literature review reveals a diverse landscape of innovative antenna designs utilizing advanced materials and fabrication techniques for various applications, from wearables to 5G communication. Building upon this foundation, our manuscript introduces a novel approach to antenna enhancement. Leveraging anodizing and Stöber methods, we aim to push the boundaries of achievable parameters. Unlike existing studies, our focus extends to a comparative analysis with flexible PET and PVC antennas, providing valuable insights into the performance of these materials under our proposed methods. This unique contribution positions our manuscript at the forefront of antenna research, offering a fresh perspective on enhancing antenna functionality through novel fabrication approaches.

2. MATERIALS AND METHODS

2.1. Chemical Procedure for Preparing of Substrates

The utilization of a metal oxide layer in antenna applications is favored owing to its specific dielectric constant and corrosion resistance [19-21]. Employing metal surfaces oxidized through the anodizing process is thus imperative. This technique enhances the lifespan of the antenna system, providing additional benefits such as improved stability in challenging climatic conditions, enhanced electrical performance, and increased durability. In this study, the anodizing technique was applied to generate oxide layers on Nickel (Ni) and 6063 Aluminum (Al) substrates. A two-electrode setup was employed for this process, with a Platinum (Pt) sheet serving as the counter electrode. The electrolyte solution comprised 0.1 M potassium hydroxide (KOH) supplemented with 50g/L of sodium tetraborate. All chemical reagents were procured from Aldrich and used without further modification. The preparation of solutions was meticulously executed using distilled water. The anodizing process was conducted under a voltage of 2V for 5 minutes. The resulting anodized substrates were designated as *Antenna-1* and *Antenna-2* for Ni and Al, respectively. Notably, substrates *Antenna-3*, *Antenna-4*, and *Antenna-5* were High-Density Polyethylene (HDPE), Polyethylene Terephthalate (PET), and another PET variant, respectively. Substrate *Antenna-6* was Aluminum coated with Silicon Dioxide (SiO_2). The SiO_2-coated Aluminum was prepared using the Stöber method, named after its inventor Werner Stöber. This widely employed technique involves synthesizing silica (SiO_2) coatings on diverse substrates. In this method, the silicon alkoxide precursor, typically tetraethylorthosilicate (TEOS), undergoes hydrolysis and condensation reactions in the presence of water and an alcohol solvent, such as ethanol or methanol, under basic conditions [22,23]. The resultant silica nanoparticles spontaneously assemble into a dense coating on the substrate surface, driven by their elevated surface energy and propensity to aggregate. The Stöber method offers notable advantages, including simplicity, scalability, and controllability, facilitating precise customization of coating thickness, particle size, and surface morphology. Additionally, the resulting coatings demonstrate high uniformity, purity, and strong adhesion to the substrate, rendering them suitable for diverse applications [24-27]. In the experimental procedure, 1.5 mL of tetraethylorthosilicate (TEOS), 1.7 mL of ammonia, 1 mL of deionized water, and 50 mL of isopropanol were combined in the reaction vessel. The mixture was maintained at a temperature of 0 °C for 15 minutes, followed by pH measurement. If the pH value deviated from the range of 10.5 to 11.5, additional ammonia was introduced to adjust the pH. Subsequently, the ice bath was removed, and the solution was subjected to magnetic stirring for 3 hours at 40 °C. After this period, an additional 1 mL of TEOS was introduced, and the reaction proceeded under identical conditions for an additional 2 hours. Following the synthesis of SiO_2 nanoparticles, the solution containing the nanoparticles underwent centrifugation at 9000 rpm for 5 minutes at 25 °C. Subsequently, the particle and liquid phases were separated, and the particles were washed twice with ethanol and acetone before being dried at room temperature. The produced SiO_2 was mixed with epoxy, serving as a binder, and the coating was applied to the surface using the spray coating technique with a spray gun. The composite coating material was introduced into the coating chamber and applied manually with a pressure gun (5-8 bar). The coated Aluminum substrate was then dried in an oven at 160 °C for 15 minutes and designated as the *Antenna-6* substrate. The morphological analysis of the antenna was conducted through SEM-EDX analysis. Field emission scanning electron microscopy (FE-SEM) measurements were carried out using an FEI Quanta 650 at 5 keV with an Energy Dispersive X-ray (EDX) detector.

2.2. Design and Analysis of Tulip-Shaped Microstrip Antenna (TSMA)

CST Microwave Studio (CST MWS) stands as a computer-aided electromagnetic simulation software designed for engineers and researchers engaged in microwave and radio frequency (RF) design. The software empowers users to conduct electromagnetic field simulations, a pivotal aspect for comprehending and optimizing the behavior of electromagnetic waves within the microwave and RF frequency spectrums. Its applications extend across diverse domains, including antenna design, microwave circuit analysis, and the performance evaluation of RF and microwave devices. Users of CST MWS can construct 2D and 3D geometries to model electromagnetic challenges, encompassing antennas, circuit elements, microwave components, and other electromagnetic structures. The software incorporates various electromagnetic simulation solvers, such as time-domain and frequency-domain solvers, facilitating the analysis of changes in electromagnetic fields over time and frequency, respectively. A distinctive feature of CST MWS is its provision of tools for parameter optimization and performance analysis during the design phase. This functionality proves instrumental in evaluating and enhancing the design's alignment with specified criteria. The software further supports seamless integration with other engineering tools and accommodates diverse data formats, thereby facilitating efficient data sharing across design stages and research environments. In order to achieve cost-effectiveness in the designed antenna, appropriate substrate materials with relative dielectric constants of 2.4, 3.5, and 4.0, and loss tangents of approximately 0.02, 0.018, and 0.019 have been selected for PLA, PET, and PVC, respectively. The dielectric material thickness is fixed at h = 1.0 mm. The dimensions of the feed line in the conventional antenna, as illustrated in Figure 1, along with those of the rectangular patch and other parameters, were determined through mathematical calculations utilizing the transmission line model. A Python software code was developed to execute these computations. Subsequently, the conventional antenna design was implemented using CST software, employing the calculated dimensions. Figures 1 presents views of the patch on both the front and back sides of the traditional microstrip patch antenna, while Table 1 provides the dimension parameters.

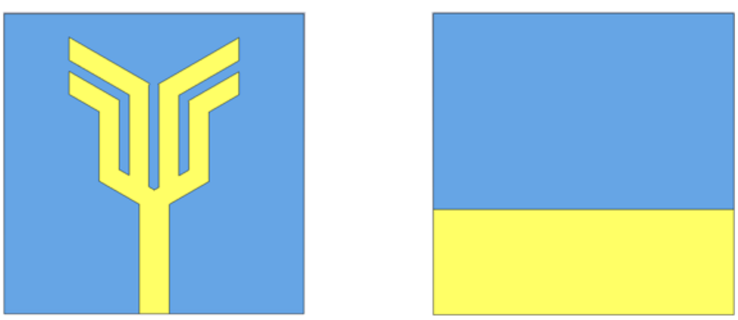

(a) (b)

Figure 1. Front view (a) and back view (b) of the simulation design of the Tulip-shaped microstrip antenna

Table 1. Parameters of TSMA

Parameters	Values
Substrate dielectric permittivity (ε_r)	PLA (2.4), PET (3.5), PVC (4.0)
Substrate thickness (h)	1 mm
Patch or copper thickness (t)	0.035 mm
Substrate length (SL)	30 mm
Substrate Width (SW)	30 mm
Feed length (FL)	3 mm
Feed Width (FW)	11 mm
Ground length (GL)	30 mm
Ground width (GW)	10. 5 mm
Ground Gap	0.5 mm

The optimization carried out in the simulation environment, as illustrated in Figure 2, reveals a notable improvement in performance when employing layer thicknesses of 1.0 mm for PLA, PET, and PVC materials compared to trials with a thickness of 1.6 mm. Subsequent analyses were conducted based on this optimized thickness value.

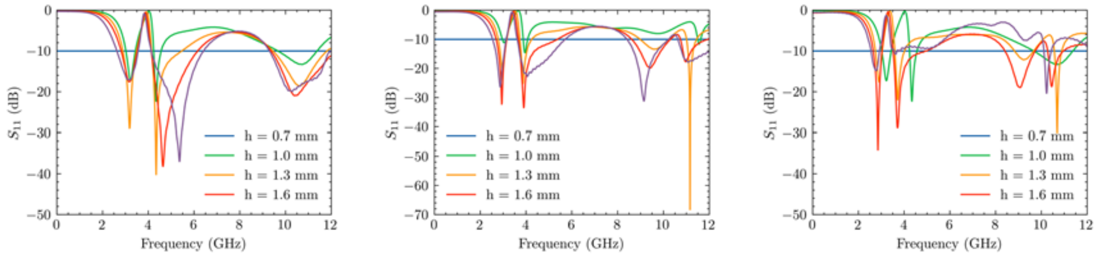

(a) **(b)** **(c)**

Figure 2. Comparison of $|S_{11}|$ curves of TSMA antenna for substrates with dielectric constants of (a) 2.4, (b) 3.5 and (c) 4 for four different thicknesses

As depicted in Figure 3, the simulated $|S_{11}|$ of the triple-resonant antenna fall within the frequency ranges of 2 GHz to 4 GHz, 4 GHz to 6 GHz, and 10 GHz to 12 GHz, respectively (when $|S_{11}|$ is below -10 dB). This observation indicates that the proposed antenna demonstrates a broad impedance bandwidth within the high-frequency band.

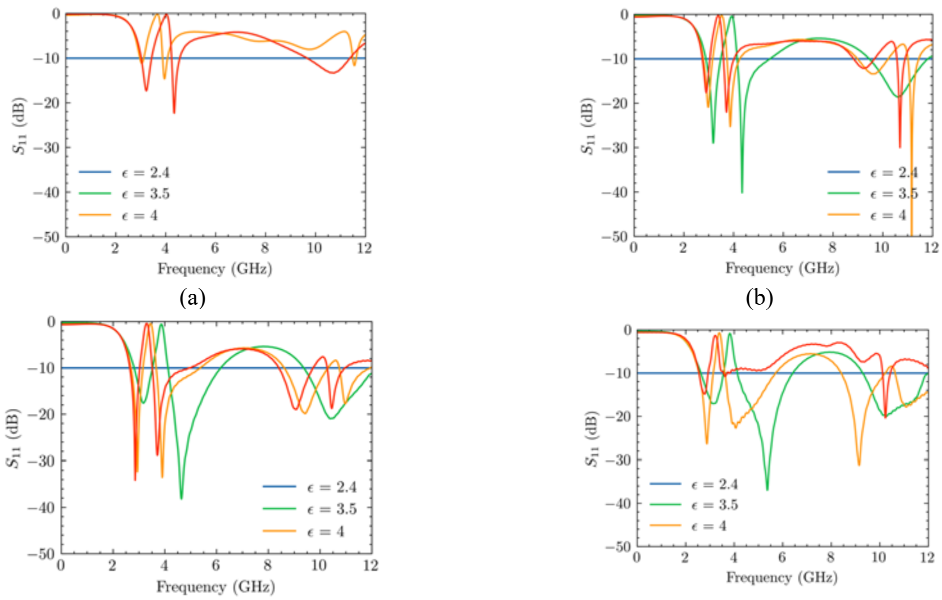

(c) (d)

Figure 3. Comparison of $|S_{11}|$ curves of TSMA for three different dielectric constants and substrate thicknesses of (a) 0.7 mm, (b) 1.0 mm, (c) 1.3 and (d) 1.6 mm

3. RESULTS AND DISCUSSIONS

Although various materials were employed for the antenna substrates, the radiating element was fashioned using cost-effective and readily manufacturable copper tape. Challenges inherent in the precise cutting of copper tape, such as tearing, were mitigated by the use of a cutting tool, ensuring the successful fabrication of the tulip-shaped antenna patches, as illustrated. Figure 4 sequentially showcases antennas fabricated from 1 to 6, while Figure 5 delineates the measurement setup.

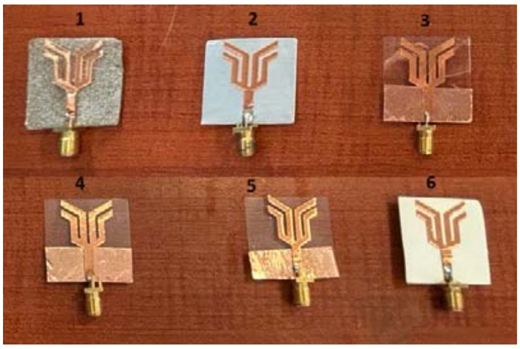

Figure 4. Photographs of fabricated Tulip-shaped microstrip antennas.

Figure 5. Measurement setup

The identical antenna geometry was constructed utilizing the materials outlined in Table 2.

Table 2. Materials of TSMA

Antenna Name	Material
Antenna-1	Ni
Antenna-2	Al
Antenna-3	HDPE
Antenna-4	PET
Antenna-5	PET
Antenna-6	SiO_2 coated Al

Figures 6 and 7 present the measured parameter graphs for S_{11} and VSWR, respectively, corresponding to the fabricated antennas. *Antenna-1* exhibits a signal attenuation trend beyond 4.5 GHz, generally falling below -5 dB. This attenuation, although exceeding the resonance reference of -3 dB indicative of functional power radiation, still maintains functionality, with approximately 68.38% of power being radiated. While optimal performance necessitates over 90% power radiation (-10 dB), the observed -5 dB level suggests satisfactory functionality, albeit not at peak performance. Notably, a tri-band performance is discernible around 6 GHz, 9.5 GHz, and 12.5-14.5 GHz, as substantiated by VSWR measurements. *Antenna-2* displays a comparable attenuation shift, reaching approximately -5 dB at 2.5 GHz. Noteworthy is its wideband performance spanning 4 GHz to 8 GHz, aligning well with applications such as 5 GHz Wi-Fi communication, 5.8 GHz drone control, and WiMAX frequency usage. This characteristic renders *Antenna-2* suitable for these purposes, a conclusion corroborated by VSWR analysis. *Antenna-3* exhibits attenuation approaching -5 dB beyond roughly 3 GHz, with fluctuations around -10 dB after 8 GHz. Although potential modifications could enhance its bandwidth performance, it tends to remain below -10 dB inconsistently near 9 GHz. Despite this, its ability to sustain power radiation around -10 dB within this range suggests effective utilization of approximately 90% of incoming power. A narrowband performance is also evident around 4 GHz, indicating its primary utility lies in applications beyond 8 GHz, as affirmed by VSWR analysis. *Antenna-4* demonstrates a tri-band performance, featuring two bands around 4 GHz and a resonant point near 9 GHz. Despite appearing narrowband, this resonance offers a bandwidth of roughly 2 GHz around -10 dB, making it suitable for sensor applications with an acceptable Q-factor. Additionally, bands spanning 4-5 GHz hold potential for sensor application use, as validated by VSWR analysis. *Antenna-5* exhibits unacceptable performance before 8 GHz, improving beyond this threshold to approximately -10 dB and further below. Wideband performance between 8 GHz and 15 GHz suggests suitability for applications within this frequency range, as confirmed by VSWR analysis. *Antenna-6* showcases performance fluctuating around -5 dB near 4 GHz, with brief drops below -10 dB around 10 GHz within a narrow bandwidth. While suitable for this frequency range, its usability for frequencies outside this range may be limited, necessitating modifications. VSWR analysis supports this observation. In summary, the primary objective of this study was to eliminate dependence on commercial products or existing materials in the production of antennas tailored to desired frequency ranges or purposes, while also providing a wide range of options for producing antennas suitable for specific purposes. From this perspective, the results of the designed antennas and the necessary analyses conducted are quite satisfactory both in terms of antenna performance and material analysis, thus making a significant contribution to the literature.

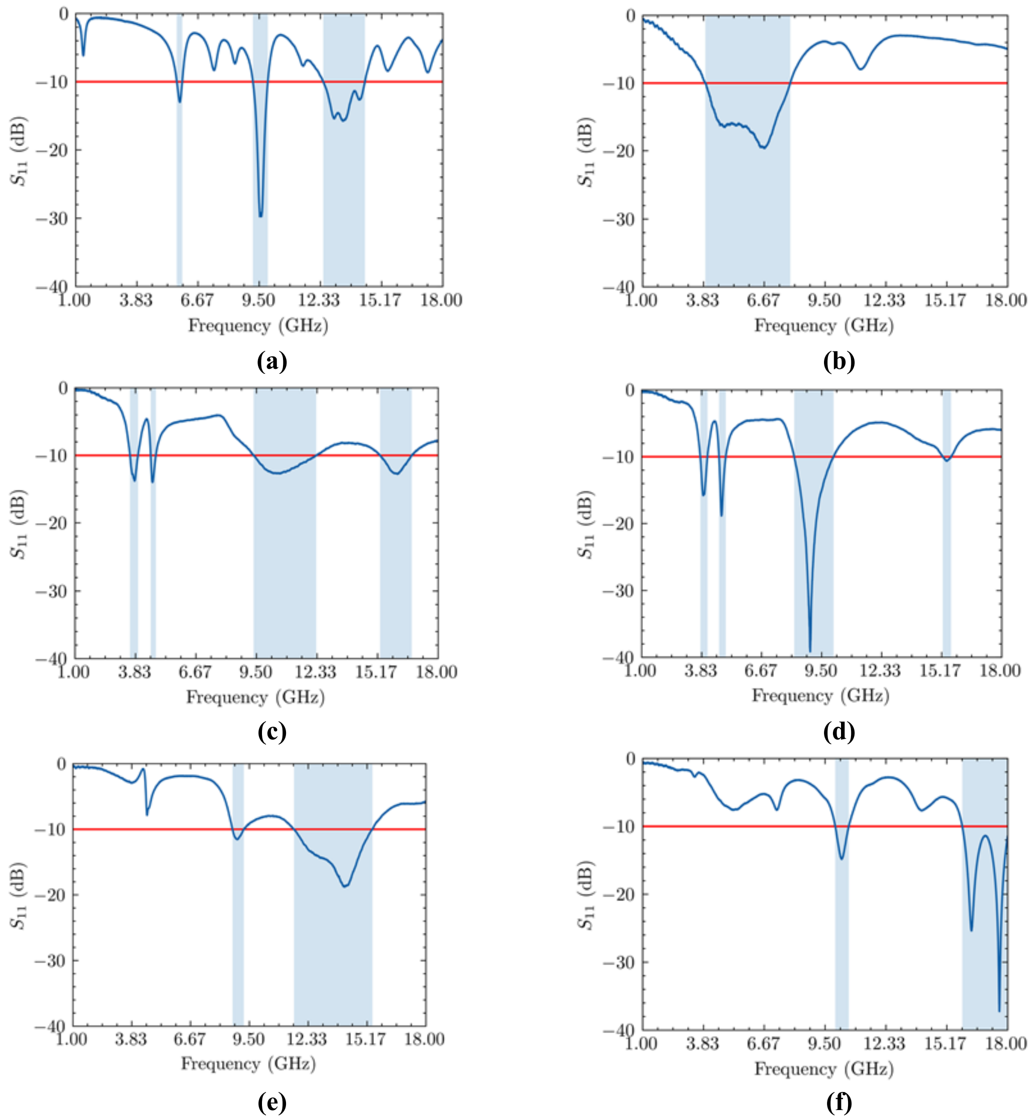

Figure 6. Measured S_{11} parameters of fabricated antennas of antenna (a) #1, (b) #2, (c) #3, (d) #4, (e) #5 and (f) #6

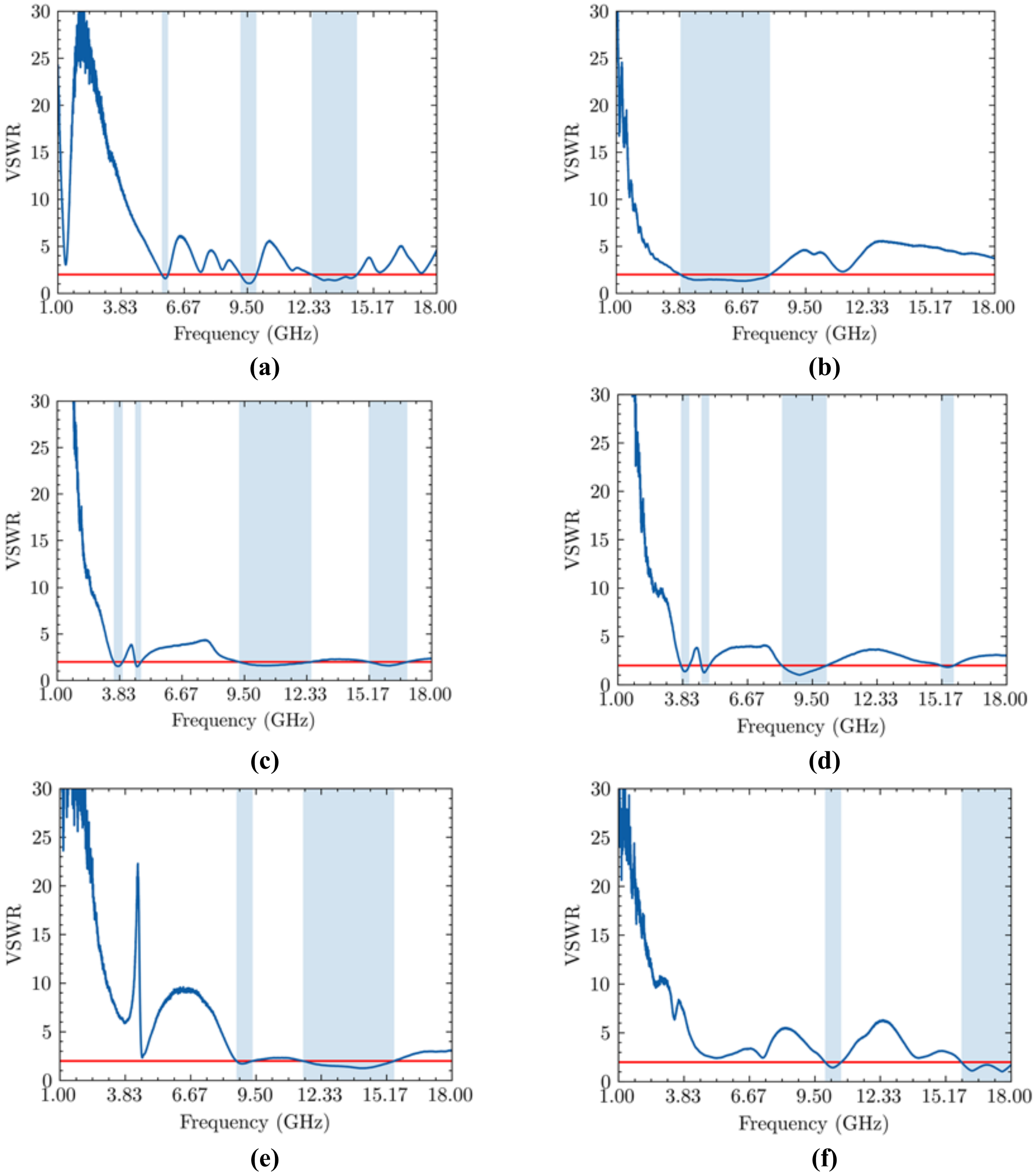

Figure 7. Measured VSWR (Voltage Standing Wave Ratio) parameters of fabricated antennas antenna (a) #1, (b) #2, (c) #3, (d) #4, (e) #5 and (f) #6

SEM and EDX analyses provide high-resolution imaging capabilities and elemental composition information, making them essential tools for identifying morphological structures. The morphological analysis of antennas 1, 2, and 6 was conducted through SEM-EDX analysis, and the results obtained are presented in Figure 8.

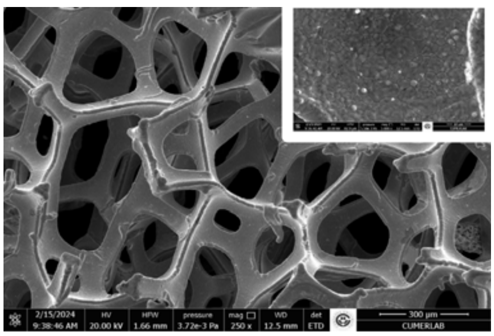

(a)

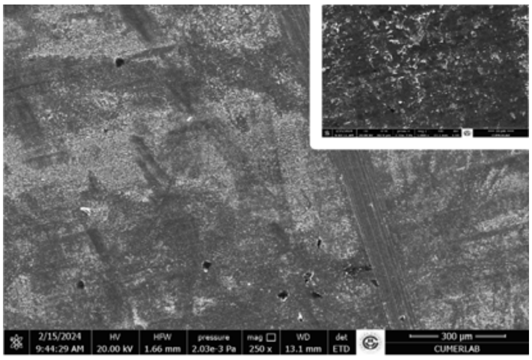

(b)

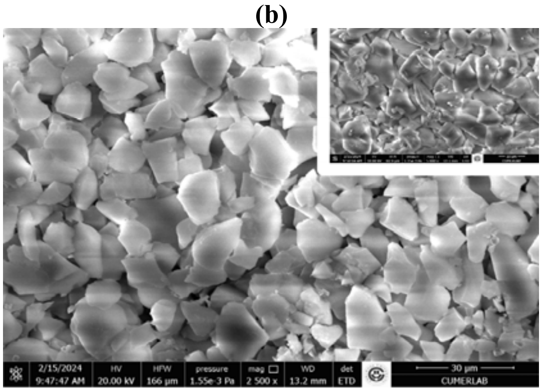

(c)

Figure 8. The SEM micrograph of (a) *Antenna-1*, (b) *Antenna-2* and (c) *Antenna-6*.

The EDX analysis of these antennas were presented in Figure 9.

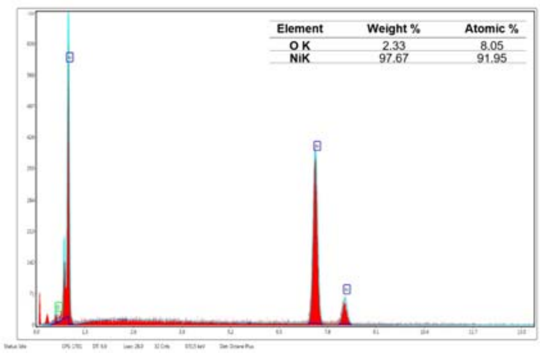

(a)

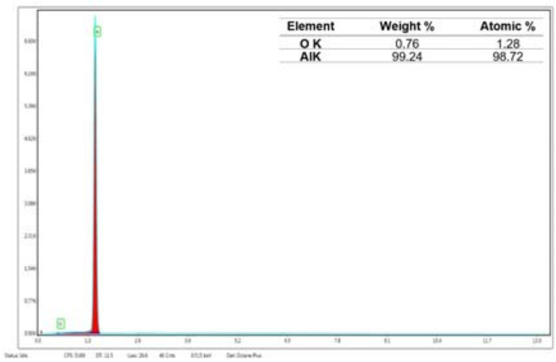

(b)

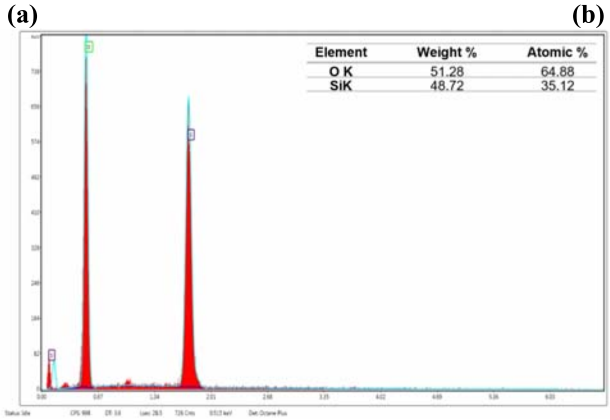

(c)

Figure 9. The EDX results of (a) *Antenna-1*, (b) *Antenna-2* and (c) *Antenna-6*.

As illustrated in Figure 8, the substrate of *Antenna-1* exhibits a complex arrangement characterized by interwoven structures, attributed to the cage-network configuration of Ni foam. This intricate design is further enriched by the presence of NiO, a byproduct of the anodizing process. The introduction of NiO significantly impacts the dielectric constant in comparison to Ni alone, imparting distinct advantages to the substrate material. The resultant oxide layer underwent detailed examination through EDX analysis, as presented in Figure 9. The weight percent of Ni in NiO was determined to be 97.67%, confirming the presence of the oxide layer. In the SEM micrograph of *Antenna-2*, the pickling effect of anodizing is distinctly evident, particularly in regions exhibiting the highest magnitude, where a homogeneous surface is detected. EDX results indicate that the alkaline environment of the anodizing solution yielded a relatively thin oxide layer, with the Al weight ratio measuring 99.24%. The SEM analysis of the *Antenna-6* substrate corroborates the presence of a SiO_2 structure, aligning with observations in existing literature. The substrate manifests as an irregular and granular structure, resembling the typical granular arrangement formed by the random aggregation of small grains/particles. Figure 9 further details the Si ratio, quantifying it as 48.72%. This comprehensive examination using SEM and EDX analyses provides valuable insights into the structural and elemental composition of the antenna substrates, offering a foundation for in-depth discussions on their material properties and potential applications.

4. CONCLUSIONS

An antenna with a distinctive tulip-shaped design, employing microstrip-fed technology, is introduced in this study. The antenna is meticulously crafted on diverse substrates, each produced through specific chemical processes utilizing flexible plastic materials. The selection of substrates is guided by a thorough material analysis, considering their impact on electromagnetic properties. The examined materials encompass anodized Ni, Al, HDPE, PET, and SiO_2-coated Al. Section 2 provides a detailed exposition of the results obtained from material analysis, elucidating the unique capabilities of the proposed antenna structure on each substrate. The findings indicate the antenna's adeptness in achieving various functionalities, including single-band, multi-band, narrow, or wideband characteristics, with commendable precision. The versatility in operating frequencies, coupled with the ease of production and compactness, positions the proposed antenna structure as highly suitable for GHz applications. These applications span a broad spectrum, encompassing material detection, material characterization, as well as GHz, microwave, and communication applications. This study contributes to the expanding repertoire of antenna designs tailored for diverse electromagnetic requirements in contemporary high-frequency applications.

5. REFERENCES

1. Avşar Aydın, E. (2017). The effect of limestone in breast cancer detection by microwaves. *Çukurova University Journal of the Faculty of Engineering and Architecture, 32*(2), 37-44.
2. Avşar Aydın, E. & Biçer, M.B. (2023). A novel frequency-configurable patch antenna design using flexible substrates for biomedical applications. *Cukurova University Journal of the Faculty of Engineering, 38*(2), 411-420.
3. Li, J., Wang, A., Qin, J., Zhang, H., Ma, Z. & Zhang, G. (2021). Lightweight polymethacrylimide@ copper/nickel composite foams for electromagnetic shielding and monopole antennas. *Composites Part A: Applied Science and Manufacturing*, *140*, 106144.
4. Bala, M., Shivling, V.D. & Tyagi, S. (2024). Tailoring the characteristics of nickel ferrite based composite for tuning the microwave absorption performance. *Materials Chemistry and Physics*, *312*, 128630.
5. Liu, Q., Huang, X., He, X., Li, X., Liu, X. & Li, Z. (2021). Flexible, breathable, and highly environmental-stable Ni/PPy/PET conductive fabrics for efficient electromagnetic interference shielding and wearable textile antennas. *Composites Part B: Engineering*, *215*, 108752.
6. Guerchouche, K., Herth, E., Calvet, L.E., Roland, N. & Loyez, C. (2017). Conductive polymer based antenna for wireless green sensors applications. *Microelectronic Engineering*, *182*, 1-8.
7. Jeon, H., Jin, S. & Shin, K.Y. (2022). Highly flexible, high-performance radio-frequency antenna based on free-standing graphene/polymer nanocomposite film. *Applied Surface Science*, *582*, 152455.
8. Feili, D., Pagel, N., Ngo, V.L., Schwarz, P. & Seidel, H. (2010). Cu based patch antenna on polymer substrate for flexible wireless sensor systems applications. *Procedia Engineering*, *5*, 268-271.
9. Hasan, I.H., Hamidon, M.N., Ismail, A., Ismail, I., Azhari, N.A.M. & Kusaimi, M.A.M. (2019). Nickel zinc ferrite thick film with linseed oil as organic vehicle for microwave device applications. *Materials Chemistry and Physics*, *236*, 121790.

10. Li, F., Li, Y.X., Liu, X. & Wen, Q. (2022). Nickel-modified zinc molybdate low temperature co-fired ceramics for two-dimensional beam splitting of array antenna in X-band. *Ceramics International*, *48*(23), 35682-35690.

11. Kyovtorov, V., Georgiev, I., Margenov, S., Stoychev, D., Oliveri, F. & Tarchi, D. (2017). New antenna design approach – 3D polymer printing and metallization: experimental test at 14–18 GHz. *AEU - International Journal of Electronics and Communications*, *73*, 107-114.

12. Anilkumar, T., Madhav, B.T.P., Rao, M.V. & Nadh, B.P. (2020). Bandwidth reconfigurable antenna on a liquid crystal polymer substrate for automotive communication applications. *AEU - International Journal of Electronics and Communications*, *117*, 153096.

13. Matyas, J., Slobodian, P., Munster, L., Olejnik, R. & Urbanek, P. (2017). Microstrip antenna from silver nanoparticles printed on a flexible polymer substrate. *Materials Today: Proceedings*, *4*(5), 5940-5944.

14. Sid, A., Cresson, P.Y., Joly, N., Braud, F. & Lasri, T. (2023). Bio-based substrate for flexible electronics - application to a 2.45 GHz wearable patch antenna. *Materials Today Electronics*, *5*, 100049.

15. Hwang, I.J., Oh, J.I., Jo, H.W., Kim, K.S., Yu, J.W. & Lee, D.J. (2022). 28 GHz and 38 GHz dual-band vertically stacked dipole antennas on flexible liquid crystal polymer substrates for millimeter-wave 5G cellular handsets. *IEEE Transactions on Antennas and Propagation*, *70*(5), 3242-3252.

16. Mohamadzade, B., Simorangkir, R.B.V.B., Hashmi, R., Lalbakhsh, A., Shrestha, S., Zhadobov, M. & Sauleau, R. (2021). A conformal, dynamic pattern-reconfigurable antenna using conductive textile-polymer composite. *IEEE Transactions on Antennas and Propagation*, *69*(10), 6175-6184.

17. Elmobarak Elobaid, H.A., Abdul Rahim, S.K., Himdi, M., Castel, X. & Abedian Kasgari, M. (2017). A transparent and flexible polymer-fabric tissue UWB antenna for future wireless networks. *IEEE Antennas and Wireless Propagation Letters*, *16*, 1333-1336.

18. Hamouda, Z., Wojkiewicz, J.L., Pud, A.A., Kone, L., Bergheul, S. & Lasri, T. (2018). Magnetodielectric nanocomposite polymer-based dual-band flexible antenna for wearable applications. *IEEE Transactions on Antennas and Propagation*, *66*(7), 3271-3278.

19. Yamasaki, K., Taniho, H., Tate, K. & Ohtsu, N. (2021). Electrolyte effect in pulsed anodization of NiTi alloy to form a Ni-free oxide layer. *Surface and Coatings Technology*, *417*, 127221.

20. Abedini, M. & Hanke, S. (2023). Improving the wear resistance of aluminum by a nickel-filled anodized porous alumina layer. *Wear*, *522*, 204858.

21. Gasco-Owens, A., Roche, J. & Arurault, L. (2024). Nanocontrolled thinning of the barrier layer thickness of porous anodic films using galvanodynamic polarization of aluminum alloys. *Electrochimica Acta*, *479*, 143894.

22. Sivolapov, P., Myronyuk, O. & Baklan, D. (2022). Synthesis of Stober silica nanoparticles in solvent environments with different Hansen solubility parameters. *Inorganic Chemistry Communications*, *143*, 109769.

23. Wulfert-Holzmann, P., Settelein, J. & Giffin, G.A. (2021). Influence of the specific surface area of Stöber silica additives on the electrochemical properties of negative electrodes in lead-acid batteries. *Journal of Energy Storage*, *34*, 102193.

24. Fernandes, R.S., Raimundo, I.M. & Pimentel, M.F. (2019). Revising the synthesis of Stöber silica nanoparticles: A multivariate assessment study on the effects of reaction parameters on the particle size. *Colloids and Surfaces A: Physicochemical and Engineering Aspects*, *577*, 390-399.

25. Yan, Y., Fu, J., Xu, L., Wang, T. & Lu, X. (2016). Controllable synthesis of SiO2 nanoparticles: Effects of ammonia and tetraethyl orthosilicate concentration. *Micro & Nano Letters*, *11*(12), 853-857.

26. Ho, V.T.T., Hong, N.V.H., Nguyen, A.V., Bach, L.G. & Dinh, T.P. (2018). Core–Shell Fe@SiO2 nanoparticles synthesized via modified Stöber method for high activity in Cr(VI) reduction. *Journal of Nanoscience and Nanotechnology*, *18*(10), 6981-6987.

27. Alam, M.A., Samad, U.A., Sherif, E.M., Poulose, A.M., Mohammed, J.A., Alharthi, N. & Al-Zahrani, S.M. (2020). Influence of SiO2 content and exposure periods on the anticorrosion behavior of epoxy nanocomposite coatings. *Coatings*, *10*(2), 118.